In Vivo Electron Transport

Observation of In Vivo Cytochrome-Based Electron-Transport Dynamics Using Time-Resolved Evanescent Wave Electroabsorption Spectroscopy**

Toshihiko Shibanuma, Ryuhei Nakamura, Yuichiro Hirakawa, Kazuhito Hashimoto, and Kazuyuki Ishii**

As biological processes consist of intricate chains of various chemical reactions, one of the central goals of life science is to clarify these reactions from a molecular-dynamics perspective to better understand the processes of life. Flash photolysis using fast laser pulses is the best technique for studying chemical reactions with minimal limitations related to time-resolution. This technique has provided important insights into the crucial details of several dynamic photoactive processes, such as electron and energy transfer in photosynthesis.[1] To photochemically control photo-inactive proteins, the coordination of CO to hemes has been employed as a photochemical tool, as the iron-bound CO ligand dissociates from hemes upon visible-light irradiation. Using the coordination of CO to isolated heme proteins, such as myoglobin, hemoglobin, cytochromes, and cytochrome c oxidase, real-time studies of protein dynamics have been widely conducted to examine the exchange of axial ligands, protein folding, and electron transfer between active sites.[2] Among the numerous critical metabolic processes, cellular respiration, which includes the electron-transport system, is particularly important for the generation of chemical energy, primarily in the form of ATP. Since in vivo respiratory electron-transport systems are thermodynamically open and consist of many proteins interacting with each other,[3] the direct application of flash photolysis to intact living cells will aid in the understanding of the molecular dynamics of in vivo respiratory electron-transport chains.

Herein, we demonstrate that time-resolved evanescent wave electroabsorption (TREWEA) spectroscopy can be applied to the direct observation of respiratory electron-transport dynamics based on c-type cytochromes (c-Cyts) in the metal-reducing bacterium *Shewanella loihica* PV-4.[4] To accomplish this observation, the following techniques were employed: 1) For direct investigation of in vivo respiratory electron-transport dynamics of bacteria, we applied the artificial photochemical reaction of CO to the bacterium *S. loihica* PV-4 (Figure 1a). In this system, respiration is inhibited by blockage of the redox activities of hemes upon CO binding but can be subsequently reactivated by photo-
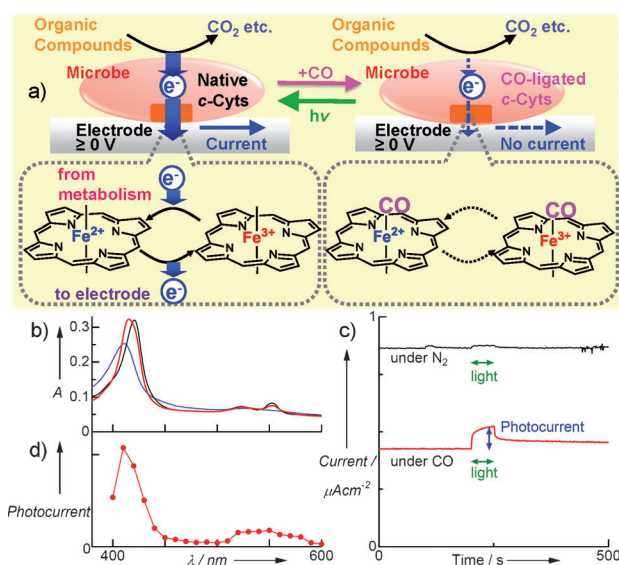
[*] Prof. Dr. K. Hashimoto, Prof. Dr. K. Ishii
HASHIMOTO Light Energy Conversion Project, ERATO/JST
4-6-1 Komaba, Meguro-ku, Tokyo 153-8904 (Japan)

T. Shibanuma, Dr. R. Nakamura, Y. Hirakawa
Department of Applied Chemistry, School of Engineering
The University of Tokyo (Japan)

Prof. Dr. K. Hashimoto
Department of Applied Chemistry, School of Engineering
The University of Tokyo
7-3-1 Hongo, Bunkyo-ku, Tokyo 113-8656 (Japan)
E-mail: hashimoto@light.t.u-tokyo.ac.jp

Prof. Dr. K. Ishii
Institute of Industrial Science, The University of Tokyo
4-6-1 Komaba, Meguro-ku, Tokyo 153-8505 (Japan)
E-mail: k-ishii@iis.u-tokyo.ac.jp

Figure 1. a) Concept for the photocontrol of microbial metabolic processes that involve extracellular electron transfer toward an electrode via c-Cyts. b) DT UV/Vis spectra of whole cells of *S. loihica* PV-4 suspended in a DM-L solution (see the Supporting Information) under N_2 (black), O_2 (blue), and CO (red) atmospheres. c) Time courses of microbial current at an electrode potential of 0.4 V (vs. a standard hydrogen electrode (SHE)) under N_2 (black) and CO (red) atmospheres. Green arrows indicate the light irradiation period. d) An action spectrum of the microbial current recovered by visible-light irradiation under a CO atmosphere (red). The action spectrum was obtained by both subtraction of the photocurrent without CO and subsequent normalization of the spectrum according to the quantity of irradiating photons.

dissociation of CO.[2f] 2) To distinguish between single photo-chemical reaction dynamics and in vivo respiratory electron-transport dynamics, secondary artificial control between active and inactive electron-transport chains should be appended to the analysis, in addition to the photochemical control. Herein, the employed bacterium *S. loihica* PV-4 can transfer electrons generated by metabolic processes to extracellular electrodes via *c*-Cyts (microbial current),[5] but it can generate the microbial current only when the electrode potential is suitable to accept electrons from *c*-Cyts.[6] Thus, the respiratory electron-transport dynamics in living cells can be controlled electrochemically, and the microbial current can be directly measured. 3) Evanescent wave (EW) electro-absorption spectroscopy, which allows the selective monitoring of molecules at an electrode surface, has been shown to be useful for investigating the electrogenic bacteria,[5a, 7] as *c*-Cyts at the cytoplasmic membrane of living cells can be spectro-scopically observed owing to both their large quantity and intense visible absorption band. By applying flash photolysis to the EW electroabsorption spectroscopy, we directly investigated the electron-transfer dynamics from bacterial metabolism to the electrode via outer membrane (OM) *c*-Cyts.

Figure 1b shows diffuse-transmission (DT) UV/Vis spectra of cell suspensions under N_2, O_2, and CO atmospheres. The Soret (419 nm) and Q (522 and 552 nm) absorption bands can be seen under N_2, which are almost identical to the OM decaheme *c*-Cyts purified from strain MR-1, and thus are attributable to in vivo ferrous (Fe^{2+}) *c*-Cyts in the cytoplasmic membrane.[5,8] Under O_2, the Soret (411 nm) and Q (ca. 525 nm) bands attributable to in vivo ferric (Fe^{3+}) *c*-Cyts are observed.[5,8] Upon treatment of in vivo ferrous (Fe^{2+}) *c*-Cyts with CO gas, the Soret band clearly shifted from 419 to 415 nm (Figure 1b), which is attributed to the coordination of CO to *c*-Cyts (Fe^{2+}) in living bacterial cells, as suggested by comparison with reports on the CO derivatives of isolated *c*-Cyts.[2d,e] However, the observed spectral changes did not occur for in vivo ferric (Fe^{3+}) *c*-Cyts, which indicates that the CO ligand cannot coordinate to ferric (Fe^{3+}) *c*-Cyts in our system.

Figure 1c shows time courses of the microbial current generated under N_2 and CO atmospheres. After injecting a dense microbial culture into an electrochemical cell with an indium tin oxide (ITO) electrode under N_2, the current rapidly increased and subsequently stabilized at approximately 0.8 $\mu A\,cm^{-2}$. The microbial current originates from electrons supplied from NADH, which is continuously generated by microbial metabolic processes (i.e., conversion of lactate→pyruvate→acetyl-CoA, or an incomplete tricar-boxylic acid (TCA) cycle), to the electrode via the electron-transport system consisting of quinol derivatives and *c*-Cyts in the inner and outer membranes.[9] Upon treatment of the cells with CO, the microbial current decreased by half (Figure 1c). This result indicates that the formation of CO-ligated *c*-Cyts (Fe^{2+}) in living cells inhibits the extracellular electron-transfer reactions of *S. loihica* PV-4. It is noteworthy that the large drop in microbial current caused by CO was reversed upon visible-light irradiation; however, visible-light irradiation induced little change in current generation under N_2 (Figure 1c). To clarify the origin of the light-induced current

recovery, excitation-wavelength dependency was investigated (Figure 1d). The action spectrum is well-correlated with the absorption spectrum of in vivo CO-ligated *c*-Cyts (Fe^{2+}), thus indicating that the current recovery arising from visible-light irradiation originates from the photodissociation of the CO ligand. This dissociation generates redox-active *c*-Cyts and revives the cellular respiratory electron-transport reactions (Figure 1a).[2f] Thus, our findings demonstrate the successful artificial control of the in vivo electron-transport chain of bacterial metabolism by the photochemistry of CO-ligated *c*-Cyts (Figure S3 in the Supporting Information).

To selectively observe the dynamics of microbial electron transfer to the electrode, a TREWEA spectroscopy system was constructed using an optical waveguide coated with an ITO electrode film (Figure S1 in the Supporting Information).[5a] In this system, *c*-Cyts at a few 100 nm from the electrode surface were selectively detected, since the penetration depth that the EW field decayed to 1/e was set up to be approximately 110 nm at a wavelength of 400 nm. The electron-transfer dynamics observed at the electrode surface can be described in terms of two possible scenarios distinguished by the midpoint potential (+0.15 V vs. SHE), at which concentrations of ferric (Fe^{3+}) and ferrous (Fe^{2+}) *c*-Cyts are similar at the electrode surface.[5a] In the first scenario, no electron is transferred to the electrode and no microbial current is generated (Figure 2d, red, the electrode potential is −0.1 V vs. SHE). This situation is similar to the dynamics observed by conventional time-resolved absorption measurements without the electrode (Figure S4 in the Supporting Information): The CO-ligated *c*-Cyts (Fe^{2+}) (415 nm) are immediately converted to the five-coordinated *c*-Cyts (Fe^{2+}) (ca. 433 nm) after laser excitation,[2d,e] and subsequently the regeneration of CO-ligated *c*-Cyts (Fe^{2+}) ($\tau_1 = 2 \times 10^{-4}$ s
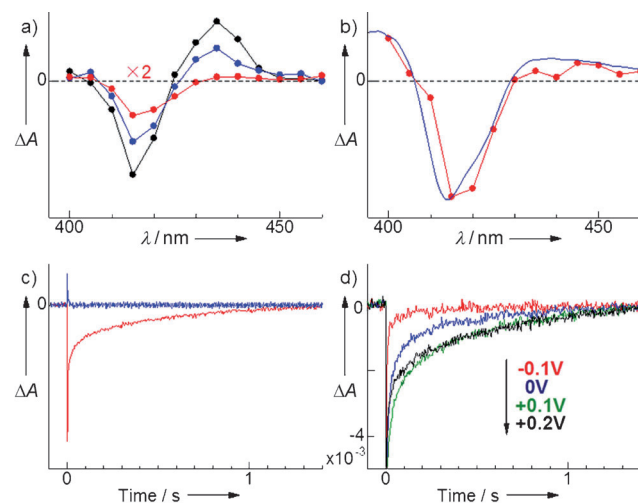

Figure 2. TREWEA of *S. loihica* PV-4 cells under a CO atmosphere. a) TREWEA spectra at 100 µs (black), 1 ms (blue), and 50 ms (red) after laser excitation (0.15 V vs. SHE). b) A TREWEA spectrum at 100 ms (red, 0.15 V) and a spectral simulation calculated from the sum of a bleaching spectrum of CO-ligated *c*-Cyts and absorption spectra of ferric (Fe^{3+}) and ferrous (Fe^{2+}) *c*-Cyts (blue). c) Time profiles of the TREWEA signals (red 415 nm, blue 435 nm; 0.15 V). d) Electrode potential dependency of TREWEA signals (415 nm).

$\approx 80\%$, $\tau_2 = 7 \times 10^{-3}$ s $\approx 20\%$) is essentially complete within 20 ms. In the second scenario, the electrode potential is set to accept electrons from microbes and generate a microbial current ($+0.1$ to $+0.3$ V vs. SHE). Here, ferric (Fe^{3+}) c-Cyts are formed as a result of transferring electrons to the electrode. At an early stage following laser excitation, bleaching (415 nm) and absorption (435 nm) signals were detected, which indicate the photodissociation of CO and formation of the five-coordinated c-Cyts (Fe^{2+}), respectively (Figure 2a). However, after 50 ms, only the bleaching signal at 415 nm was observed. The time profiles of the bleaching and absorption signals revealed that the former has a slow decay component ($\tau = 5 \times 10^{-1}$ s), whereas the latter disappears without the slow component ($\tau = 2 \times 10^{-4}$ s, Figure 2c). Notably, the dependency of the slow component on the electrode potential indicates that the signal intensity increases in the following order: -0.1 V (ca. 0) $\ll 0$ V < 0.1–0.2 V, while the signal lifetime is independent of the electrode potential ($0 - +0.3$ V; Figure 2d). Thus, the slow decay of bleaching was observed at 415 nm only when the respiratory electron-transport chain was active and generating a current.

In this slow process, ferric (Fe^{3+}) c-Cyts, which are formed after the electron transfer to the electrode, are expected to be a key intermediate, since time-resolved current measurements indicate that electron transfer from in vivo ferrous (Fe^{2+}) c-Cyts to the electrode is essentially complete within a few milliseconds after the photodissociation of CO (Figure S5 in the Supporting Information). In fact, the TREWEA spectrum of the slow component at the midpoint potential ($+0.15$ V vs. SHE) is well-reproduced by taking into account the formation of ferric (Fe^{3+}) c-Cyts in addition to the disappearance of CO-ligated c-Cyts (Fe^{2+}) and the formation of ferrous (Fe^{2+}) c-Cyts (Figure 2b). The disappearance of ferric (Fe^{3+}) c-Cyts corresponding to the slow decay of bleaching results from reduction of ferric (Fe^{3+}) to ferrous (Fe^{2+}) c-Cyts, and subsequent recombination with CO (the CO ligand does not coordinate to ferric (Fe^{3+}) c-Cyts in our system). As the recombination with CO is complete within 20 ms without electron transfer to the electrode, the rate of reduction to ferrous (Fe^{2+}) c-Cyts represents the rate-determining step of disappearance of ferric (Fe^{3+}) c-Cyts. Therefore, the slow decay ($\tau = 5 \times 10^{-1}$ s) reflecting the activity of respiratory electron-transport chain is attributable to the rate of metabolic reduction reaction of ferric (Fe^{3+}) c-Cyts, such as electron transfer from quinol derivatives to ferric (Fe^{3+}) c-Cyts in the inner membrane, or from ferrous (Fe^{2+}) c-Cyts in the inner membrane to ferric (Fe^{3+}) c-Cyts in the OM (Figure 3). Since the process of electron transfer from ferrous (Fe^{2+}) c-Cyts to the electrode is complete within a few milliseconds, the rate-determining step in electron transport from cells to the electrode is the reduction of ferric (Fe^{3+}) c-Cyts ($\tau = 5 \times 10^{-1}$ s).
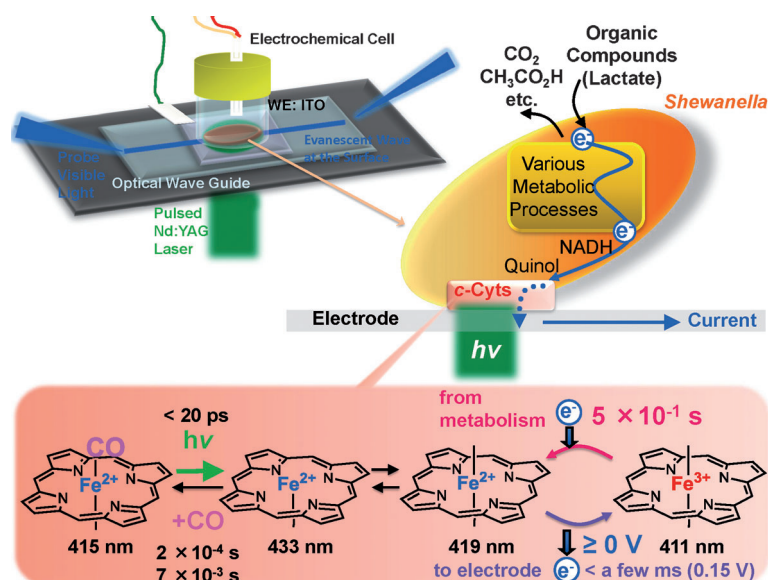

Figure 3. Summary of the photodynamics of *S. loihica* PV-4 under a CO atmosphere and the TREWEA system. The CO-ligated c-Cyts (Fe^{2+}) are immediately converted to the five-coordinated ferrous (Fe^{2+}) c-Cyts after laser excitation. When the electrode potential is suitable to accept the electrons from microbes and generate a microbial current, ferric (Fe^{3+}) c-Cyts are formed as a result of transferring electrons to the electrode. In the case of *Shewanella*, electrons supplied from NADH continuously generated by metabolic processes are transferred to ferric (Fe^{3+}) c-Cyts via quinol derivatives.[9]

In summary, we showed the usefulness of TREWEA spectroscopy for investigating in vivo respiratory electron-transport dynamics of electrogenic bacteria treated with the photochemical tool, CO. The overall view of electron-transfer dynamics presented herein is useful for the detailed understanding of respiratory energy generation in living cells, particularly because of the increasing interest in microbial metabolic processes involving electron transfer between cells and extracellular substrates, such as minerals and electrodes.[10] Together with previous biochemical investigations of photoactive living systems involving photosynthetic reactions, our approach of applying flash photolysis to photo-inactive intact cells is an important first step in pioneering a new field of spectroscopic studies of the rapid dynamics of living systems.

Experimental Section

S. loihica PV-4 was pre-cultivated aerobically in Marine Broth (10 mL; 20 gL^{-1}) at 30°C for 24 h. Subsequently, the culture was centrifuged, and then the pelleted cells were cultivated aerobically at 30°C for two days in defined media containing lactate [DM-L; NaHCO$_3$ (2.5 gL^{-1}), CaCl$_2$·2H$_2$O (0.08 gL^{-1}), NH$_4$Cl (1.0 gL^{-1}), MgCl$_2$·6H$_2$O (0.2 gL^{-1}), NaCl (10 gL^{-1}), 2-[4-(2-hydroxyethyl)-1-piperazinyl]ethanesulfonic acid (HEPES, 7.2 gL^{-1})] and yeast extract (0.5 gL^{-1} as a microelement growth supplement).[5a, 6] To harvest cells, the culture suspension was centrifuged for ten minutes, and the pelleted cells were washed three times with DM-L before they were used for experiments. Coordination of CO to c-Cyts in living cells was achieved by passing CO gas through the cell suspension of *S. loihica* PV-4.

DT UV/Vis spectra of intact cells of *S. loihica* PV-4 in a sealed quartz cuvette (1 mm optical path length) were recorded on a Shimadzu UV-2550 spectrometer equipped with an integrating sphere (MPC-2200).[5a] Current generated from *S. loihica* PV-4 was monitored by a single-chamber, three-electrode system with lactate as the carbon source and electron donor (Figure S1 in the Supporting Information). Pt wire and Ag/AgCl (KCl sat.) electrodes were used as counter and reference electrodes, respectively.[5a, 6] An ITO electrode was used as a working electrode and was set at the bottom of the reactor. DM-L (4 mL) was deaerated by bubbling N_2 gas through it (>20 min). At a constant potential of 0.4 V (25 °C, pH 7.8), a cell suspension in DM-L (0.2 mL) was injected into a reactor using a syringe, and the current output was then measured using a potentiostat system (HSV-100, Hokuto Denko). Here, the initial OD_{600} value in the reactor was adjusted to 2. For the photocurrent measurements, a Xe lamp (Asahi Spectra MAX-302) was used as an excitation source to irradiate light from the bottom of the electrochemical cell. An action spectrum was measured by interference filters that produce monochromatic light (full width at half maximum 10 nm). The TREWEA spectroscopy system was constructed with a quartz optical waveguide coated by an ITO electrode film (System Instruments) as a working electrode (Figure 3 and Figure S1 in the Supporting Information).[5a] A single-chamber electrochemical reactor was mounted onto the ITO substrate and sealed with a silicon rubber O-ring. An Ag/AgCl (KCl sat.) electrode and a platinum wire were used as the reference and counter electrodes, respectively. The incident light from a metal-halide lamp (Sigma Koki IMH-250) or a Xe lamp (Asahi Spectra LAX-103) was inclined at an angle of about 8° from the surface of the ITO substrate. The light was detected by a monochromator (JASCO CT-25TP) and a photomultiplier (Hamamatsu Photonics R928). By using a digital oscilloscope (Iwatsu-LeCroy LT342), time profiles of the photomultiplier signals in the Soret band regions were recorded point by point at 5 nm intervals. Here, a Nd:YAG laser (Spectra Physics INDI-40, 532 nm, ca. 5 mJ pulse^{-1}) was used for excitation.

[1] a) J.-L. Martin, J. Breton, A. J. Hoff, A. Migus, A. Antonetti, *Proc. Natl. Acad. Sci. USA* **1986**, *83*, 957; b) G. S. Engel, T. R. Calhoun, E. L. Read, T.-K. Ahn, T. Mančal, Y.-C. Cheng, R. E. Blankenship, G. R. Fleming, *Nature* **2007**, *446*, 782.

[2] a) U. Liebl, G. Lipowski, M. Négrerie, J.-C. Lambry, J.-L. Martin, M. H. Vos, *Nature* **1999**, *401*, 181; b) A. Ostermann, R. Waschipky, F. G. Parak, G. U. Nienhaus, *Nature* **2000**, *404*, 205; c) M. Lim, T. A. Jackson, P. A. Anfinrud, *Science* **1995**, *269*, 962; d) C. M. Jones, E. R. Henry, Y. Hu, C.-K. Chan, S. D. Luck, A. Bhuyan, H. Roder, J. Hofrichter, W. A. Eaton, *Proc. Natl. Acad. Sci. USA* **1993**, *90*, 11860; e) D. B. O'Connor, R. A. Goldbeck, J. H. Hazzard, D. S. Kliger, M. A. Cusanovich, *Biophys. J.* **1993**, *65*, 1718; f) E. Tazawa, A. Fujiwara, I. Yasumasu, *Comp. Biochem. Physiol. Part B* **1991**, *99*, 207.

[3] H. Tributsch, L. Pohlmann, *Science* **1998**, *279*, 1891.

[4] Y. Roh et al., *Appl. Environ. Microbiol.* **2006**, *72*, 3236.

[5] a) R. Nakamura, K. Ishii, K. Hashimoto, *Angew. Chem.* **2009**, *121*, 1634; *Angew. Chem. Int. Ed.* **2009**, *48*, 1606; b) Y. Xiong, L. Shi, B. Chen, M. U. Mayer, B. H. Lower, Y. Londer, S. Bose, M. F. Hochella, J. K. Fredrickson, T. C. Squier, *J. Am. Chem. Soc.* **2006**, *128*, 13978; c) L. Shi, T. C. Squier, J. M. Zachara, J. K. Fredrickson, *Mol. Microbiol.* **2007**, *65*, 12; d) C. R. Myers, J. M. Myers, *J. Bacteriol.* **1992**, *174*, 3429; e) R. S. Hartshorne, B. N. Jepson, T. A. Clarke, S. J. Field, J. Fredrickson, J. Zachara, L. Shi, J. N. Butt, D. J. Richardson, *J. Biol. Inorg. Chem.* **2007**, *12*, 1083.

[6] a) G. J. Newton, S. Mori, R. Nakamura, K. Hashimoto, K. Watanabe, *Appl. Environ. Microbiol.* **2009**, *75*, 7674; b) A. Okamoto, R. Nakamura, K. Ishii, K. Hashimoto, *ChemBioChem* **2009**, *10*, 2329.

[7] J. P. Busalmen, A. Esteve-Núñez, A. Berná, J. M. Feliu, *Angew. Chem.* **2008**, *120*, 4952; *Angew. Chem. Int. Ed.* **2008**, *47*, 4874.

[8] a) Circular dichroism and magnetic circular dichroism suggest that most of the *c*-Cyt proteins of *S. loihica* PV-4 have two histidine residues as axial ligands (Figure S2 in the Supporting Information); b) Y. Takayama, Y. Kobayashi, N. Yahata, T. Saitoh, H. Hori, T. Ikegami, H. Akutsu, *Biochemistry* **2006**, *45*, 3163; c) R. M. M. Branca, G. Bodó, Z. Várkonyi, M. Debreczeny, J. Ősz, C. Bagyinka, *Arch. Biochem. Biophys.* **2007**, *467*, 174; d) S. J. Field, P. S. Dobbin, M. R. Cheesman, N. J. Watmough, A. J. Thomson, D. J. Richardson, *J. Biol. Chem.* **2000**, *275*, 8515.

[9] a) Y. J. Tang, A. L. Meadows, J. D. Keasling, *Biotechnol. Bioeng.* **2007**, *96*, 125; b) Y. J. Tang, A. L. Meadows, J. Kirby, J. D. Keasling, *J. Bacteriol.* **2007**, *189*, 894; c) L. Shi, D. J. Richardson, Z. Wang, S. N. Kerisit, K. M. Rosso, J. M. Zachara, J. K. Fredrickson, *Environ. Microbiol. Rep.* **2009**, *1*, 220.

[10] a) Y. A. Gorby et al., *Proc. Natl. Acad. Sci. USA* **2006**, *103*, 11358; b) D. R. Lovley, *Nat. Rev. Microbiol.* **2006**, *4*, 497; c) G. Reguera, K. D. McCarthy, T. Mehta, J. S. Nicoll, M. T. Tuominen, D. R. Lovley, *Nature* **2005**, *435*, 1098; d) S. K. Lower, M. F. Hochella Jr. , T. J. Beveridge, *Science* **2001**, *292*, 1360.